Baltic Astronomy, vol. 9, 59–68, 2000.

MODE IDENTIFICATION IN PULSATING WHITE DWARFS USING THE HST

S. O. Kepler[1], E. L. Robinson[2], D. Koester[3], J. C. Clemens[4], R. E. Nather[5] and X. J. Jiang[6]

[1] *Instituto de Física da Universidade Federal do Rio Grande do Sul, 91501-970 Porto Alegre, RS, Brazil*

[2] *McDonald Observatory and Department of Astronomy, University of Texas, Austin, TX 78712-1083, U.S.A.*

[3] *Institut für Astronomie und Astrophysik, Universität Kiel, D-24098 Kiel, Germany*

[4] *Department of Physics, University of North Carolina, Chapel Hill, NC 27599-3255, U.S.A.*

[5] *McDonald Observatory and Department of Astronomy, University of Texas, Austin, TX 78712-1083, U.S.A.*

[6] *Beijing Astronomical Observatory and United Laboratory of Optical Astronomy, Chinese Academy of Sciences, Beijing 100101, China*

Received November 17, 1999

Abstract. We obtained time-resolved ultraviolet spectroscopy for the pulsating DA stars G 226-29 and G 185-32 and for the pulsating DBV star PG 1351+489 with the Hubble Space Telescope Faint Object Spectrograph, to compare the ultraviolet to the optical pulsation amplitudes. We find that for essentially all observed pulsation modes the amplitude rises to the ultraviolet just as the theoretical models predict for $\ell = 1$ modes. We do not find any pulsation mode visible only in the ultraviolet, as expected if high ℓ pulsations were excited.

Key words: stars: oscillations, individual: G 226-29, PG 1351+489, G 185-32

1. INTRODUCTION

A crucial step in determining the structure of a white dwarf from its pulsation periods is to identify the pulsation modes correctly. The pulsation modes are indexed with three integers (k,ℓ,m) where k represents the number of nodes in the pulsation eigenfunction along the radial direction, ℓ is the number of node lines on the stellar surface and m gives the orientation of the lines. Pulsation modes with different indices generally have different pulsation periods. The usual procedure for identifying the mode indices is (1) calculate theoretical pulsation periods for white dwarf models; (2) compare the pattern of theoretical periods to the observed pattern of periods; (3) adjust the models to bring the theoretical and observed patterns into closer agreement. The problems with this procedure are clear: it does not work for white dwarfs with only a few excited pulsation modes, as it places too few constraints on the stellar structure; and, given the complexity and sophistication of the theoretical calculations and the large number of possible pulsation modes, there is ample opportunity to misidentify modes. Other methods of mode identification must be used to avoid these problems.

2. MODE IDENTIFICATION USING TIME-RESOLVED UV SPECTROSCOPY

Time-resolved ultraviolet spectroscopy provides an independent method for determining pulsation indices of white dwarfs. The amplitudes of g-mode pulsations depend strongly on ℓ at wavelengths shorter than 3000 Å. Fig. 1 shows how the amplitude depends on wavelength and ℓ for the lowest-order modes of a pulsating DA white dwarf. The amplitude of all modes increases towards the ultraviolet but the amplitude increases more for $\ell = 2$ than for $\ell = 1$. The differences are even greater for modes with higher ℓ.

The increase of amplitude from optical to the ultraviolet is caused by two effects: the increasing effect of the temperature on the flux but also the increasing effect of limb darkening to the ultraviolet. The differences between the amplitudes of modes with different ℓ are caused mainly by limb darkening. The brightness variations of non-radially pulsating white dwarfs are due entirely to variations in effective temperature; geometric variations are negligible (Robinson, Kepler & Nather 1982). The pulsations divide the stellar surface into zones of higher and lower effective temperature described by

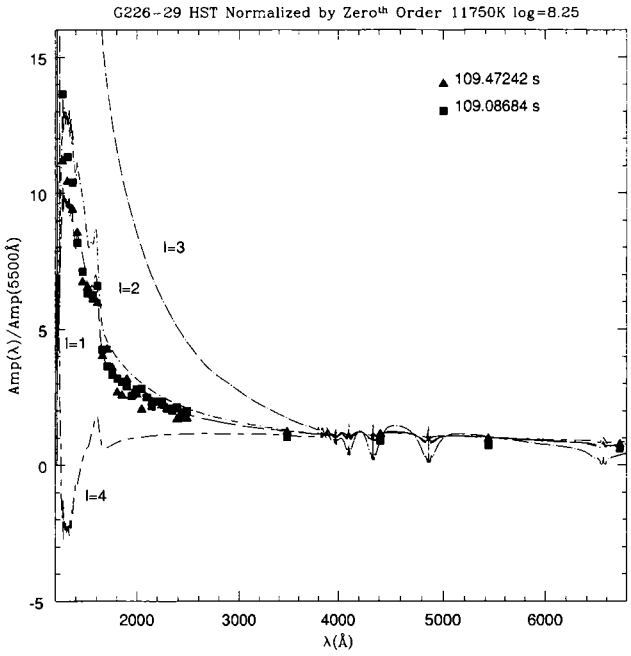

Fig. 1. The amplitudes of the $\ell = 1$ to $\ell = 4$ pulsation modes in a pulsating DA white dwarf as a function of wavelength. The atmospheres were calculated from the most recent version of the model atmosphere code by Koester (Finley, Koester & Basri 1997). The points are the measured amplitudes of the two main periodicities of G 229-29.

spherical harmonics; modes of higher ℓ have more zones than those of lower ℓ. From a distance, we can measure only the integrated surface brightness, which includes the effects of limb darkening, so modes of higher ℓ are normally washed out by the cancellation of different zones. But at ultraviolet wavelengths, the effects of limb darkening increase drastically, decreasing the contribution of zones near the limb. Consequently, modes of higher ℓ are cancelled less effectively in the UV and their amplitudes increase more steeply at short wavelengths than those of low ℓ. Theoretical calculations of the amplitudes require good model atmospheres but are entirely independent of the details of pulsation theory and white dwarf structure calculations.

Robinson et al. (1995) used this method to determine ℓ for the pulsating DA white dwarf G 117-B15A. They measured the amplitude of its 215 s pulsation in the ultraviolet with the HST high-speed

photometer and identified it as an $\ell = 1$ mode. Equipped with the correct value of ℓ, they found that the mass of the surface hydrogen layer in G 117-B15A was between 1.0×10^{-6} and $8 \times 10^{-5}\ M_{\odot}$, which is too thick to be consistent with models invoking thin hydrogen layers to explain the spectral evolution of white dwarfs. They also found $T_{\rm eff} = 12,375 \pm 125$ K, substantially lower than the accepted temperature at that time but close to the presently accepted temperature (Koester et al. 1994, Bergeron et al. 1995).

To extend the results, we observed the pulsating DA white dwarfs G 226-29 (DN Dra) and G185-32 (PY Vul) and the DBV star PG 1351+489 (EM UMa) with 10 s exposure RAPID mode of the Faint Object Spectrograph (FOS) of the Hubble Space Telescope. We used the blue Digicon detector and the G 160L grating over the spectral region 1150 Å to 2510 Å.

3. ZERO ORDER DATA

Even though not much advertised by the STScI, the zeroth order light from the object falls onto the detector for the G 160L grating (Eracleous & Horne 1996). It consists of *simultaneous* photometry of the object with an effective wavelength around 3400 Å. The data should be extracted from pixels 620 to 645 from the c4 files. As all the pulsating white dwarfs are multiperiodic, for all our data, the zeroth order light was crucial as a measurement of the amplitude at 3400 Å, sampled exactly as the time resolved spectra. As the zeroth order light has a counting rate around 100 times larger than the total light collected on the time resolved spectra, its statistical properties are of higher quality, and can be used to search for low amplitude pulsations. None undetected previously were found for any star observed in this project. Even though the central wavelength of the mirror is uncertain, the amplitude vs. wavelength changes only by a few percent for 100 Å, so we include the uncertainty in the wavelength as an uncertainty in the normalization.

The calibration pipeline of the HST data contains a transmission curve for the zeroth order data measured on the ground prior to launch, but our data are inconsistent with such transmission curve, which should present an amplitude of pulsation much larger than observed, according to the same models that predict the ultraviolet amplitudes observed. The ultraviolet efficiency of the mirror must be much lower than measured on the ground, but the effective wave-

length is consistent with our measurements, within an uncertainty of around 100 Å.

4. G 226-29

G 226-29, also called DN Dra, LP 101 – 148 and WD 1647+591, is the brightest known pulsating DA white dwarf (DAV or ZZ Ceti star), with $V = 12.22$. At just over 12 pc, it is the closest ZZ Ceti star (optical parallax of 82.7 ± 4.6 mas, Harrington & Dahn 1980; Hipparcos parallax of 91.1 ± 2.1 mas, Vauclair et al. 1997). The star was discovered to pulsate by McGraw & Fontaine (1980), using a photoelectric photometer attached to the MMT telescope. They found a periodicity at 109 s and 6 mma amplitude. Kepler, Robinson & Nather (1983) used time-series photometry to solve the light curve and interpret the variations as an equally spaced triplet with periods near 109 s. The outer peaks have similar amplitudes, near 3 mma, and are separated by $\delta f = 16.14\,\mu$Hz from the central peak, which has an amplitude of 1.7 mma. These results were confirmed by Kepler et al. (1995), using the Whole Earth Telescope, and no other pulsation was found up to a detection limit of 0.4 mma. G 226-29 has the simplest mode structure, the second smallest overall pulsation amplitude, and the shortest dominant period of any pulsating white dwarf, making it a unique object.

G226-29 was observed with the HST six times, each time for 3 hours, between September 1994 and December 1995. As the star is bright and fairly hot, the summed spectrum from each 3-hour observation has a high signal-to-noise ratio.

5. PG 1351+489

PG 1351+489 is the DBV with the simplest pulsation spectrum, and therefore the one which requires the shortest data set to measure its amplitude. It was discovered to pulsate by Winget, Nather & Hill (1987), with a dominating period at 489 s and peak-to-peak amplitude around 0.16 mag. The light curve also present the first and second harmonic plus peaks at $1.47\,f_0$, $2.47\,f_0$ and $3.47\,f_0$, with low amplitudes. We observed PG 1351+489 for 4 consecutive orbits of HST, with a total of 2.67 h on the star. The ultraviolet and zeroth order spectra show only the 489 s and its harmonic at 245 s above the noise, with an indication that a peak at 599 s marginally significant on both Fourier spectra. A fit of the normalized ultraviolet ampli-

tudes to the theoretical ones, for the main periodicity at 489 s and its harmonic at 245 s, fit an $\ell = 1$ mode, with $T_{\rm eff} = 22\,500\,{\rm K} \pm 250\,{\rm K}$, and $\log g = 8.0 \pm 0.10$, or an $\ell = 2$ mode with $T_{\rm eff} = 23\,100\,{\rm K} \pm 250\,{\rm K}$ and $\log g = 7.5 \pm 0.10$. But if we require the temperature to be consistent with the time-average spectra itself, only the $\ell = 1$ mode fits the 489 s periodicity wavelength dependence of the amplitude. The uncertainty on the 245 s periodicity prevents us from making a clear distinction between $\ell = 1$ and $\ell = 2$ for such mode.

6. G 185-32

G 185-32 was discovered as a multiperiodic pulsator by McGraw et al. (1981) with periods of 71 s, 141 s and 215 s. We observed G 185-32 for a total of 7.13 hr on July 31, 1995. Table 1 shows a fit of the pulsation amplitude (Amp) and times of maxima (T_{max}) for different wavelengths.

Table 1. G 185-32

	Ultraviolet		Zeroth Order	
Period (s)	Amp(mma)	$T_{\rm max}$(s)	Amp(mma)	$T_{\rm max}$(s)
215.7	7.81 ± 0.34	61.7 ± 1.6	2.68 ± 0.15	61.8 ± 2.0
370.1	4.66 ± 0.36	106.1 ± 4.5	2.15 ± 0.16	99.6 ± 4.3
70.9	4.48 ± 0.36	29.8 ± 0.9	1.81 ± 0.17	28.5 ± 1.0
72.5	3.18 ± 0.36	26.6 ± 1.3	1.21 ± 0.16	21.4 ± 1.6
301.3	4.22 ± 0.36	25.1 ± 4.1	1.90 ± 0.16	289.0 ± 4.0
300.0	4.14 ± 0.36	182.8 ± 4.1	1.86 ± 0.16	199.6 ± 4.1
560.0	3.37 ± 0.36	44.8 ± 9.6	1.74 ± 0.16	-1.5 ± 8.2
141.8	1.85 ± 0.37	98.3 ± 4.5	1.56 ± 0.16	103.2 ± 2.3

7. MODEL ATMOSPHERES

The model atmospheres used to determine the intensity at different angles with the surface normal, and from that the pulsation amplitude as a function of wavelength were calculated with the code of D. Koester. He uses the ML2/α=0.6 version of the standard mixing length theory of convection and include the latest version of the quasi-molecular Lyman α opacity after Allard et al. (1994).

This choice of convective efficiency allows for a consistent temperature determination from optical and ultraviolet time-average spectra (Bergeron et al. 1995, Vauclair et al. 1997, Koester & Allard 2000) and also with the wavelength dependence of the amplitude (Fontaine et al. 1996).

Table 2. Measured amplitudes for G 226-29 in mma.

λ	Amp_0	Amp_1	Amp_2
1266	20.58 ±4.44	26.20 ±4.56	43.53 ±4.56
1315	12.52 ±2.25	24.26 ±2.31	36.18 ±2.31
1364	11.56 ±1.79	22.04 ±1.83	33.15 ±1.83
1412	10.48 ±1.47	20.02 ±1.51	26.05 ±1.51
1461	7.76 ±1.15	15.78 ±1.18	22.69 ±1.18
1510	7.61 ±1.22	15.33 ±1.25	20.20 ±1.25
1559	7.52 ±1.24	14.29 ±1.27	19.96 ±1.27
1607	6.01 ±1.00	13.98 ±1.03	21.01 ±1.03
1656	4.95 ±0.79	9.42 ±0.81	13.56 ±0.81
1705	4.04 ±0.76	9.98 ±0.78	11.59 ±0.77
1753	4.04 ±0.73	8.42 ±0.75	10.62 ±0.75
1802	4.27 ±0.68	6.27 ±0.69	10.16 ±0.69
1851	3.38 ±0.65	6.00 ±0.66	9.78 ±0.66
1899	3.33 ±0.66	7.40 ±0.68	9.23 ±0.68
1948	3.48 ±0.60	6.01 ±0.62	8.10 ±0.62
1997	4.15 ±0.60	6.08 ±0.62	8.90 ±0.62
2046	3.42 ±0.56	4.80 ±0.57	8.98 ±0.57
2094	2.06 ±0.54	5.84 ±0.55	7.96 ±0.55
2143	2.38 ±0.46	5.46 ±0.48	6.88 ±0.48
2192	2.98 ±0.48	5.42 ±0.49	7.49 ±0.49
2240	1.90 ±0.47	5.14 ±0.48	7.49 ±0.48
2289	1.87 ±0.40	4.93 ±0.41	6.66 ±0.41
2338	1.92 ±0.39	4.81 ±0.40	6.38 ±0.40
2386	1.61 ±0.39	3.94 ±0.40	6.80 ±0.40
2435	1.25 ±0.36	3.98 ±0.36	6.18 ±0.36
2484	2.19 ±0.42	4.02 ±0.43	6.36 ±0.43
3480	1.61 ±0.09	2.87 ±0.09	3.25 ±0.09
4410	1.53 ±0.06	2.66 ±0.06	2.86 ±0.06
5430	1.27 ±0.08	2.30 ±0.08	2.28 ±0.08
6730	1.00 ±0.10	1.81 ±0.10	1.94 ±0.01

The amplitudes depend not only on the wavelength, but also on T_{eff} and $\log g$.

8. ULTRAVIOLET AMPLITUDES

To analyze the HST data for the pulsation time variability, we first integrated the observed spectra into one bin, by summing over all wavelengths, to get the highest signal to noise ratio. We then transformed the time base to Barycentric Julian Dynamical Time (BJDD), and obtained a Fourier transform of the intensity versus time. In all cases we conclude that the ultraviolet (HST) data sets presents only the pulsation modes previously detected.

We then proceeded with a least-squares fit of the amplitude vs. wavelength observed curves to the theoretical ones, and for G 226-29 all three modes fit an $\ell = 1$ g-mode. P_0, the central mode, can be fit with both an $\ell = 1$ or $\ell = 2$ mode because of the large uncertainties in its amplitude, caused by the spectral leakage of the P_1 and P_2 modes, and its intrinsic lower amplitude. Table 2 shows the measured amplitudes from the HST data.

We determined the ℓ, $T_{\rm eff}$, and $\log g$ independently for each of three modes, P_0, P_1 and P_2. All modes fit the same model, with $T_{\rm eff} = 11\,750 \pm 20$ K, $\log g = 8.23 \pm 0.06$. Note that the quoted uncertainties are only those of the least-squares fit and do not represent the true uncertainties. The true uncertainties are difficult to estimate because they must include not only the uncertainties due to normalization of the flux at 3400Å, the HST flux calibration, but also the uncertainties due to the mixing-length approximation used in the model atmospheres (Bergeron et al. 1995, Koester & Vauclair 1997), incapable of representing the true convection in the star at different depths (Ludwig, Jordan & Steffen 1994).

For G 185-32 and PG 1351+489 a fit of the change in amplitude with wavelength with all three parameters: $T_{\rm eff}$, $\log g$ and ℓ free resulted in ℓ being either 1 or 2, but the required temperatures and gravities for $\ell = 2$ were inconsistent with those derived from the time-averaged spectra itself. We therefore fixed the temperature and gravity to those given by the time-averaged spectra, V magnitude and parallax (Koester & Allard 2000) and fitted the amplitude variation for ℓ. $\ell = 1$ is the best fit for all the modes, except the 141 s mode of G 185-32 that does not fit any pulsation index, because its amplitude does not change significantly to the ultraviolet, as expected from the theoretical models.

It is important to note that all pulsations have the same phase at all wavelengths, to within the measurement error of a few seconds, and therefore no phase shift with wavelength is detected, assuring

that all geometric and some non-adiabatic effects are negligible [the main non-adiabatic effect is a phase shift between the motions (velocities) and the flux variation, not measurable in our data].

9. FIT TO THE AVERAGE SPECTRA OF G226-29

We used our high S/N average spectra to fit to Koester's model atmospheres, constrained by *Hipparcos* parallax (Vauclair et al. 1997) to obtain $T_{\rm eff} = (12\,015 \pm 125)\,{\rm K}$, $\log g = 8.023 \pm 0.05$. The pure spectral fitting does not constrain the $\log g$, only a narrow $T_{\rm eff}$ range. The parallax, on the other hand, very narrowly constrains the luminosity and (via the mass-radius relation) $T_{\rm eff}$, the radius and thus $\log g$.

10. DISCUSSION

For a DAV, an $\ell = 1$ mode with 109 s period requires a $k = 1$ radial index, from pulsation calculations, and therefore G 226-29 has to have a thick hydrogen surface layer, around $10^{-4} M_\star$ (Bradley 1997). The effective temperature derived from the pulsation amplitudes, $T_{\rm eff} = 11\,750\,{\rm K}$, and surface gravity $\log g = 8.23$, indicate a mass of $(0.75 \pm 0.04) M_\odot$, according to the evolutionary models of Wood (1992). Such a low temperature indicates the instability strip is at much lower temperature than previously quoted. The temperature derived from the HST spectra itself, $T_{\rm eff} = 12\,015\,{\rm K}$, fits a bit better.

We are thankful to Bob Williams, the former Director of the STScI for granting us director's discretionary time for the G 226-29 observations and to Jeffrey Hayes, our project scientist at STScI, for the continuous help with the HST data reduction. Support for this work was provided by NASA through grants from the Space Telescope Science Institute, which is operated by AURA, Inc., under NASA contract NAS5-26555. Support for this work was also provided by CNPq & FINEP-Brazil.

REFERENCES

Allard N. F., Koester D., Feautrier N., Spielfiedel A. 1994, A&AS, 108, 417

Bergeron P., Wesemael F., Lamontagne R., Fontaine G., Saffer R. A., Allard N. F. 1995, ApJ, 449, 258

Bradley P. A. 1998, in *The Fourth WET Workshop Proceedings*, eds. E. G. Meištas & P. Moskalik, Baltic Astronomy, 7, 111
Eracleous M., Horne K. 1996, ApJ, 471, 427
Finley D. S., Koester D., Basri G. 1997, ApJ, 488, 375
Fontaine G., Brassard P., Bergeron P. Wesemael F. 1996, ApJ, 469, 320.
Harrington R. S., Dahn C. C. 1980, AJ, 85,454
Kepler S. O., Robinson E.L., Nather R. E. 1983, ApJ, 271, 744
Kepler S. O., Giovannini O., Wood M. A., Nather R. E., Winget D. E., Kanaan A., Kleinman S. J., Bradley P. A., Provencal J. L., Clemens J. C., Claver C. F., Watson T. K., Yanagida K., Krisciunas K., Marar T. M. K., Seetha S., Ashoka B. N., Leibowitz E., Mendelson H., Mazeh T., Moskalik P., Krzesiński J., Pajdosz G., Zoła S., Solheim J.-E., Emanuelsen P.-I., Dolez N., Vauclair G., Chevreton M., Fremy J.-R., Barstow M. A., Sansom A. E., Tweedy R. W, Wickramasinghe D. T., Ferrario L., Sullivan D. J., van der Peet A. J., Buckley D. A. H., Chen A.-L. 1995, ApJ, 447, 874
Koester D., Allard N. F. 2000, in *The Fifth WET Workshop Proceedings*, eds. E. G. Meištas & G. Vauclair, Baltic Astronomy, 9, 119
Koester D., Allard N. F., Vauclair G. 1994, A&A, 291, L9
Koester D., Vauclair G. 1997, in *Proceedings of the 10th European Workshop on White Dwarfs*, eds. J Isern, M. Hernanz & E. Garcia–Berro, NATO ASI Series, Springer Verlag, Berlin, p. 429
Ludwig H.-G., Jordan S., Steffen M. 1994, A&A, 284, 105
McGraw J. T., Fontaine G. 1980, unpublished results
McGraw J. T., Fontaine G. Lacombe P., Dearborn D. S. P., Gustafson J., Starrfield S. G. 1981, ApJ, 250, 349
Robinson E. L., Kepler S. O., Nather R. E. 1982, ApJ, 259, 219
Robinson E. L., Mailloux T. M., Zhang E., Koester D., Stiening R. F., Bless R. C., Percival J. W., Taylor M. J., van Citters, G. W. 1995, ApJ, 438, 908
Vauclair G., Schmidt H., Koester D., Allard N. 1997, A&A, 325, 105
Winget D. E., Nather R. E., Hill J. A. 1987, ApJ, 316, 305
Wood M. A. 1992, ApJ, 386, 539